Journal of Radiation Researches, vol.11, No.1, 2024, Baku
Heat flow rate function and thermophysical properties of TiNbCN coating materials
pp. 33-39

PACS: 74.62.Dh; 74.62.Bf; 74.62.En

HEAT FLOW RATE FUNCTION AND THERMOPHYSICAL PROPERTIES OF TiNbCN COATING MATERIALS

K.M. Hasanov[1,2], I.I. Mustafayev[1], O.A. Samedov[1], R.N. Mehdiyeva[1]

[1]*Institute of Radiation Problems, MSE AR*
[2]*International Intergovernmental Organization Joint Institute for Nuclear Research, Russia*
hasanovkanan11@gmail.com

Abstract: The crystal structure and thermal properties of TiNbCN coatings were investigated in this research work. Structural investigations conducted using X-ray diffraction revealed that the crystal structure of this coating conforms to cubic phase group symmetry under normal conditions and at room temperature. Thermophysical investigations determined that thermal transitions in the TiNbCN coating occur through complex mechanisms. Analysis of the DSC (Differential Scanning Calorimetry) spectra kinetics revealed rapid decomposition below T≤50 °C, weak decomposition below T≤270 °C, and rapid decomposition above T≤600 °C. Furthermore, it was determined from the DSC kinetics that a phase transition occurs at a temperature of 565 °C.

Keywords: coating materials, heat flow rate function, crystal structure, phase analysis, DSC.

1. Introduction

In recent years, significant research efforts have been dedicated to nitride-based coatings, encompassing various types such as TiN, ZrN, TiSiN, ZrSiN, ZrTiN, ZrNbN, and ZrTiSiN. These investigations have given particular attention to the assessment of their mechanical and elastic properties, residual stress levels, corrosion resistance, and thermal stability [1-3]. Furthermore, carbide coatings, including TiC, TiSiC, TiZrC, TiNbC, and TiSiZrC, have displayed enhanced tribological performance attributed to the incorporation of amorphous carbon (a-C) acting as a solid lubricant. Additionally, these coatings exhibit favorable electrical characteristics and resistance to oxidation [4]. Noteworthy are studies conducted by Chang et al., underscoring the substantial impact of carbon content on the mechanical and wear properties of TiSiC coatings synthesized via cathodic arc evaporation. Elevated acetylene flow rates result in diminished friction coefficients [5-6]. Comparing coatings fabricated through physical vapor deposition (PVD) methods reveals widespread utilization of carbonitrides in applications demanding mechanical, tribological, and oxidation resistance. These coatings feature a "perfectly" mixed C and N in a f.c.c structure, combining the optimal characteristics of both parent components, carbide, and nitride. Notably, TiCN coatings exemplify superior mechanical resistance and thermal stability when contrasted with standalone TiC and TiN coatings. This results from the amalgamation of the high ductility and high melting point of TiC, coupled with the superior adhesion strength and low internal stress of TiN [7]. Furthermore, various configurations are available for carbonitrides, including monolayer, multilayer, or graded structures, offering precise control over structure and composition, leading to adjustable properties [8]. Among carbonitrides, ternary coatings containing a single transition metal, such as TiCN, ZrCN, NbCN, or CrCN, find extensive use in industrial applications [9]. Despite the regular commercial availability of TiCN and CrCN, ongoing extensive research is essential. In recent years, a novel generation of carbonitrides has emerged by incorporating various metallic and/or non-metallic elements into the basic ternary matrix. Constantin et al. demonstrated that introducing small amounts of Zr, Nb, or Si into TiZrCN, TiNbCN, and TiSiCN systems results in decreased stress and increased adhesion. Furthermore, corrosion processes of high-speed steel in aggressive NaCl environments were significantly improved [10]. To date, complex Ti carbonitride coatings prepared via PVD, incorporating alloying elements such as Cr and/or Si, have been explored in structures like TiCrCN, TiSiCN, TiCrNbCN, TiAlSiCN, TiCrSiCN, and TiNbCN, revealing their superior properties for diverse applications. Ensuring high oxidation resistance in Ti (C, N)-based cermets, especially around 900 °C, is crucial for applications like high-speed dry cutting. This imperative arises from the susceptibility to oxidation and subsequent tool failure during the cutting process [11-12]. At elevated temperatures, oxygen diffusion on the tool material's surface initiates a series of oxidation reactions, resulting in the formation of a loosely adherent oxide layer. This newly formed oxide layer in Ti (C, N)-based cermets compromises the strength and hardness of cermet tools, exacerbating wear and tool failure, and diminishing the stability and lifespan of the tools during cutting [13]. Significant efforts have been invested in enhancing the oxidation resistance of cermet cutting tools. Notably, the incorporation of Ta in Ti (C, N)-based cermets reduces the thickness of the oxide layer while enhancing its density. This serves to decelerate the diffusion rate of oxygen atoms at elevated temperatures, thereby improving the oxidation resistance of Ti (C, N)-based cermets [14].

2. Experimental methods

The crystal structure, phase composition, texture, and grain size of the coatings were determined through X-ray diffraction (XRD) analysis. A Rigaku SmartLab diffractometer with Cu Kα radiation (wavelength of 1.5405 nm) was utilized in a θ/2θ geometry range of 30-80° with a step size of 0.02°/min, and an incident angle of 3°. Texture and crystallite sizes were calculated based on XRD peak widths using Rietveld analysis [15-22]. The DSC measurements were carried out using the DSC3 STARe Systems manufactured by METTLER TOLEDO. The standard adiabatic calorimetry was performed in the temperature range of 300 K up to 1000 K at a heating rate of 5 K/min in an argon atmosphere at a flow rate (20 mL/min) and which was previously calibrated with indium. The cooling process was achieved with the help of the NITROGEN UN 1977 REFRIGERATED LIQUID analyzer cooling system and "digital temperature controller”.The error of weight determination did not exceed 1.02 % at 300 K and 1% at 1000 K [23-27].

3. Results and Discussion

Figure 1 depicts the diffraction spectra of the TiNbCN coating. Theoretical and experimental results for the diffraction spectra clearly characterize the coating [16]. The alpha and beta phases of the TiAlV substrate, as well as the TiC, NbC, and TiN crystal phases, were determined in various quantities. The formation of NbC crystals and the degree of TiC crystal formation are greater depending on the C/N ratio in the coating.

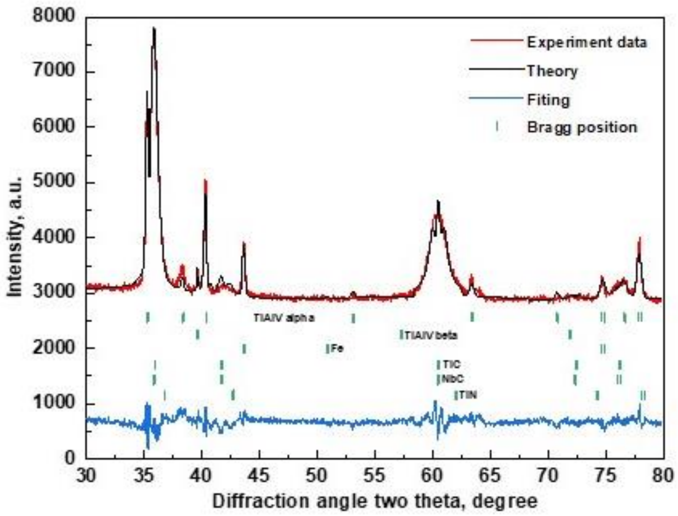

Phases	Space group	Lattice parameters of TiNbCN, Å	Cell volumes of TiNbCN, Å^3
		a, b and c (before)	
Ti_5Al_4V alpha	P 63/m m c Hexagonal	2.93409 2.93409 4.68759	34.94834
Ti_5Al_4V beta	I m -3m Cubic	3.21705	33.29462
Fe	F m -3m Cubic	3.59208	46.34863
TiC	F m -3 m Cubic	4.32856	81.10201
NbC	F d -3 m Cubic	4.33289	81.34550
TiN	F m -3 m Cubic	4.23621	76.02064

Fig. 1. Lattice parameters, space group, and cell volume of TiNbCN coating.

The interpretation of experimental data using the Rietveld package reveals that TiC, NbC, and TiN crystals form in the same cubic phase group. Additionally, it appears that NbC crystals constitute the dominant phase within the coating. The lattice parameters of NbC crystals were determined to be 4.33289 Å, with a lattice volume of 81.3455 Å^3 (Fig. 1). Figure 2 illustrates the temperature dependence of the heat flow (DSC) and the kinetics of time-temperature transformation (DTA) for the TiNbCN coating at a constant heating rate of 5 °C/min. Throughout all experimental trials, the heating rate and the flow rate of the inert Ar gas provided to the environment were kept constant within the selected temperature interval to maintain consistency in the dynamics of heat flow variation.

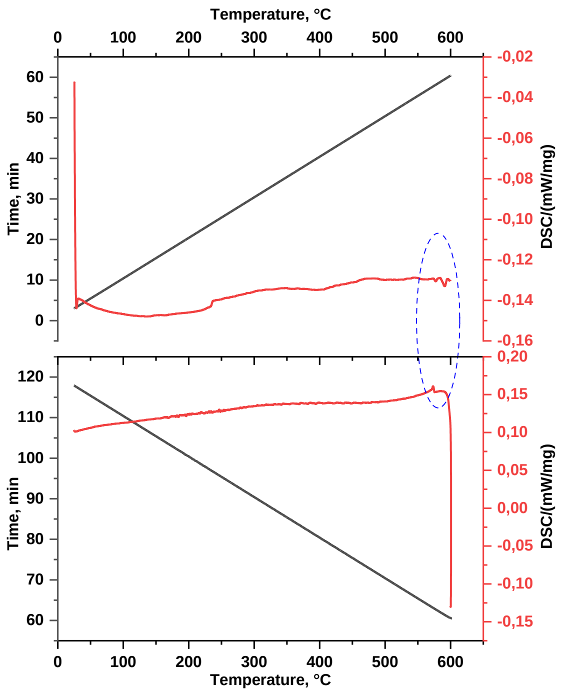

Fig. 2. DSC spectrum of the TiNbCN coating within the temperature range of 30≤T≤600 °C.

The thermal transitions occurring for the TiNbCN coating during the heating and cooling processes in the DSC spectrum can be divided into the following sections:

- T ≤ 50 °C: Rapid decomposition phase characterized by the fast degradation of adsorbed water molecules on the surface, predominantly facilitated by Ti+ elements.
- 50 ≤ T ≤ 270 °C: Decomposition of hydroxyl groups or involvement in solvothermal chemical reactions.
- 565 °C: Phase transition.

The temperature range of 30≤T≤600 °C indicates that the TiNbCN coating undergoes solvothermal reactions, leading to the thermal degradation of adsorbed water molecules on the surface predominantly by the active reducing character of the Ti+ element. The rapid phase involves the degradation of weakly interacting water molecules on the surface. The thermophysical parameters of the rapid degradation process have been determined as an enthalpy of 24.7 J/g and an energy of 256.44 mJ. At higher temperature intervals, the physical-chemical processes occurring in the structure indicate the decomposition of hydroxyl groups on the surface due to strong interactions and the involvement of active centers in the solvothermal reaction. Naturally, the decomposition of hydroxide groups, which are more active in the higher temperature range, is observed in the kinetics of these reactions. Specifically, for this transition, the change in thermophysical parameters comprises an enthalpy of 30.7 J/g and an energy of 56.59 mJ. At 565 °C, the TiNbCN coating undergoes thermal degradation, and a phase transition occurs in the mass kinetics of the sample. This phase transition serves as an experimental indicator of the occurrence of oxidation reactions. The involvement of Ti^{2+} ions in oxidation reactions with active oxygen anions is evident in this chemical conversion.

4. Conclusion

In the TiNbCN coating, TiC, NbC, and TiN crystals exhibit the same cubic phase groups.

The lattice parameters of TiC, NbC, and TiN crystals were determined to be 4.33289 Å, with a lattice volume of 81.3455 Å^3. DSC analysis has determined that during an isothermal process, the heat capacity of the TiNbCN coating remains constant in the temperature interval of 25°C to 600°C, with C/N ratio values of 0.6 and 1.6. In the TiNbCN(C/N=0.6) coating, the central peak at 590°C is observed in the heat capacity curve during both heating and cooling processes. Simultaneously, in the TiNbCN(C/N=1.6) coating, the central peak of the effect is characterized by broadening and deep endo- and exothermic effects. Furthermore, thermodynamic functions of the TiNbCN coating have been determined within the temperature range of 25°C to 600°C.

References

1. R. Mareus, C. Mastail, F. Anğay, N. Brunetière and G. Abadias, 2020. Study of columnar growth, texture development and wettability of reactively sputter-deposited TiN, ZrN and HfN thin films at glancing angle incidence. Surface and Coatings Technology, 399, p.126130.
2. P. Yi, L. Zhu, C. Dong and K. Xiao, 2019. Corrosion and interfacial contact resistance of 316L stainless steel coated with magnetron sputtered ZrN and TiN in the simulated cathodic environment of a proton-exchange membrane fuel cell. Surface and Coatings Technology, 363, pp.198-202.
3. Z. Rao and E. Chason, 2020. Measurements and modeling of residual stress in sputtered TiN and ZrN: Dependence on growth rate and pressure. Surface and Coatings Technology, 404, p.126462.
4. N. Marchin and F. Ashrafizadeh, 2021. Effect of carbon addition on tribological performance of TiSiN coatings produced by cathodic arc physical vapour deposition. Surface and Coatings Technology, 407, p.126781.
5. Q.L. Tang, Y.C. Wu, B.S. Lou, Z.Y. Chen and J.W. Lee, 2019. Mechanical property evaluation of ZrSiN films deposited by a hybrid superimposed high power impulse-medium frequency sputtering and RF sputtering system. Surface and Coatings Technology, 376, pp.59-67.
6. I.A. Saladukhin, G. Abadias, V.V. Uglov, S.V. Zlotski, A. Michel and A.J. van Vuuren, 2017. Thermal stability and oxidation resistance of ZrSiN nanocomposite and ZrN/SiNx multilayered coatings: A comparative study. Surface and Coatings Technology, 332, pp.428-439.
7. M.B. Kanoun and S. Goumri-Said, 2014. Effect of alloying on elastic properties of ZrN based transition metal nitride alloys. Surface and Coatings Technology, 255, pp.140-145.
8. M.R. Chellali, C.M. Garzón, J.J. Olaya, H. Hahn and L. Velasco, 2021. Effect of discharge current on the corrosion resistance and microstructure of ZrTiSiN coatings deposited by magnetron co-sputtering. Materials Today Communications, 26, p.102151.
9. D.M. Devia, E. Restrepo-Parra and P.J. Arango, 2011. Comparative study of titanium carbide and nitride coatings grown by cathodic vacuum arc technique. Applied Surface Science, 258(3), pp.1164-1174.
10. A.O. Eriksson, J.Q. Zhu, N. Ghafoor, M.P. Johansson, J. Sjölen, J. Jensen, M. Odén, L. Hultman and J. Rosén, 2011. Layer formation by resputtering in Ti–Si–C hard coatings during large scale cathodic arc deposition. Surface and Coatings Technology, 205(15), pp.3923-3930.
11. A. Pogrebnjak, V. Ivashchenko, O. Maksakova, V. Buranich, P. Konarski, V. Bondariev, P. Zukowski, P. Skrynskyy, A. Sinelnichenko, I. Shelest and N. Erdybaeva, 2021. Comparative

measurements and analysis of the mechanical and electrical properties of Ti-Zr-C nanocomposite: Role of stoichiometry. Measurement, 176, p.109223.
12. K.A. Kuptsov, A.N. Sheveyko, O.S. Manakova, D.A. Sidorenko and D.V. Shtansky, 2020. Comparative investigation of single-layer and multilayer Nb-doped TiC coatings deposited by pulsed vacuum deposition techniques. Surface and Coatings Technology, 385, p.125422.
13. C. Vitelaru, M. Balaceanu, A. Parau, C.R. Luculescu and A. Vladescu, 2014. Investigation of nanostructured TiSiC–Zr and TiSiC–Cr hard coatings for industrial applications. Surface and Coatings Technology, 251, pp.21-28.
14. C.L. Chang and Y.W. Chen, 2010. Effect of the carbon content on the structure and mechanical properties of Ti–Si–C coatings by cathodic arc evaporation. Surface and Coatings Technology, 205, pp. S1-S4.
15. M.N. Mirzayev, K.M. Hasanov, A.C. Parau, E. Demir, A.S. Abiyev, T. Karaman, S.H. Jabarov, M. Dinu, E.P. Popov and A. Vladescu, 2023. Effect of the C/N ratio modification on the corrosion behavior and performance of carbonitride coatings prepared by cathodic arc deposition. Journal of Materials Research and Technology, 27, pp.1724-1738.
16. M.N. Mirzayev, A.C. Parau, L. Slavov, M. Dinu, D. Neov, Z. Slavkova, E.P. Popov, M. Belova, K. Hasanov, F.A. Aliyev and A. Vladescu, 2023. TiSiCN as coatings resistant to corrosion and neutron activation. Materials, 16(5), p.1835.
17. A. Vladescu, M.N. Mirzayev, A.S. Abiyev, A.G. Asadov, E. Demir, K.M. Hasanov, R.S. Isayev, A.S. Doroshkevich, S.H. Jabarov, S. Lyubchyk and S. Lyubchyk, 2023. Effect of Si and Nb additions on carbonitride coatings under proton irradiation: a comprehensive analysis of structural, mechanical, corrosion, and neutron activation properties. Nuclear Materials and Energy, 35, p.101457.
18. E. Popov, L. Slavov, E. Demir, B.A. Abdurakhimov, A.S. Doroshkevich, O.A. Aliyev, S.H. Jabarov, A.H. Valizade, B. Mauyey, P. Horodek and K. Siemek, 2023. Microstructural evolution of TiC nano powders under fast neutron irradiation: A multi-technique analysis. Vacuum, 215, p.112338.
19. A.V. Maletskyi, T.E. Konstantinova, G.K. Volkova, D.R. Belichko, A.S. Doroshkevich, E. Popov, N. Cornei, B. Jasinska, Z.V. Mezentseva, A.A. Tatarinova and M.N. Mirzayev, 2023. High hydrostatic pressure influence on the properties and tendency to agglomeration of ZrO_2 grains of the Al_2O_3–YSZ composite ceramics system. Ceramics International, 49(10), pp.16044-16052.
20. L. Chkhartishvili, S. Makatsaria, N. Gogolidze, O. Tsagareishvili, T. Batsikadze, M. Mirzayev, S. Kekutia, V. Mikelashvili, J. Markhulia, T. Minashvili and K. Davitadze, 2023. Obtaining Boron Carbide and Nitride Matrix Nanocomposites for Neutron-Shielding and Therapy Applications. Condensed Matter, 8(4), p.92.
21. S.F. Samadov, A.S. Abiyev, A.G. Asadov, N.V.M. Trung, A.A. Sidorin, O.A. Samedov, E.P. Popov, E. Demir, T. Vershinina, Y.I. Aliyev and K.M. Hasanov, 2024. Investigating the crystal structure of ZrB_2 under varied conditions of temperature, pressure, and swift heavy ion irradiation. Ceramics International, 50(2), pp.3727-3732.
22. T.A. Darziyeva, E.S. Alekperov, S.H. Jabarov and M.N. Mirzayev, 2023. Influence of heavy ions on the magnetic properties of Fe_3O_4 nanoparticles. Integrated Ferroelectrics, 232(1), pp.127-133.
23. F.G. Agayev, S.V. Trukhanov, A.V. Trukhanov, S.H. Jabarov, G.S. Ayyubova, M.N. Mirzayev, E.L. Trukhanova, D.A. Vinnik, A.L. Kozlovskiy, M.V. Zdorovets and A.S.B. Sombra, 2022. Study of structural features and thermal properties of barium hexaferrite upon indium doping. Journal of Thermal Analysis and Calorimetry, 147(24), pp.14107-14114.

24. Mirzayev M.N., 2021. Heat transfer of hexagonal boron nitride (h-BN) compound up to 1 MeV neutron energy: Kinetics of the release of wigner energy. Radiation Physics and Chemistry, 180, p.109244.
25. M.N. Mirzayev, E. Popov, E. Demir, B.A. Abdurakhimov, D.M. Mirzayeva, V.A. Sukratov, A.K. Mutali, V.N. Tiep, S. Biira, M.Y. Tashmetov and K. Olejniczak, 2020. Thermophysical behavior of boron nitride and boron trioxide ceramics compounds with high energy electron fluence and swift heavy ion irradiated. Journal of Alloys and Compounds, 834, p.155119.
26. M.N. Mirzayev, 2020. Simultaneous measurements of heat flow rate and thermal properties of nano boron trioxide under neutron irradiation at the low and high temperature. Vacuum, 173, p.109162.
27. M.N. Mirzayev, 2020. Oxidation kinetics of boron carbide ceramic under high gamma irradiation dose in the high temperature. Ceramics International, 46(3), pp.2816-2822.

ФУНКЦИЯ ТЕПЛОВОГО ПОТОКА И ТЕПЛОФИЗИЧЕСКИЕ СВОЙСТВА МАТЕРИАЛОВ ПОКРЫТИЯ TiNbCN

К.М. Гасанов, И.И. Мустафаев, О.А. Самадов, Р.Н. Мехтиева

Резюме: Исследована кристаллическая структура и тепловые свойства покрытия TiNbCN в рамках научной работы. Исследование структуры, проведенное методом рентгеновской дифракции, показало, что кристаллическая структура этого покрытия соответствует кубической фазовой группе с нормальными условиями и комнатной температурой. Термофизические исследования показали, что тепловые переходы в покрытии TiNbCN происходят с использованием сложных механизмов. Из кинетики DSC определено, что при $T \leq 50$ °C происходит быстрое разложение, при $T \leq 270$ °C происходит слабое разложение, а при $T \leq 600$ °C снова наблюдается быстрое разложение. Кроме того, из кинетики DSC определено, что при температуре 565 °C происходит фазовый переход.

Ключевые слова: материалы покрытий, функция теплового потока, кристаллическая структура, фазовый анализ, ДСК.

TiNbCN ÖRTÜK MATERİALLARININ İSTİLİK AXINI FUNKSİYASI VƏ TERMOFİZİKİ XÜSUSİYYƏTLƏRİ

K.M. Həsənov, İ.İ. Mustafayev, O.Ə. Səmədov, R.N. Mehdiyeva

Xülasə: Tədqiqat işində TiNbCN örtüyünün kristal quruluşu və istilik xassələri tədqiq edilmişdir. Rentgen difraksiyası metodu ilə aparılmış quruluş tədqiqatları nəticəsində müəyyən edilmişdir ki, bu örtüyün kristal quruluşu normal şəraitdə və otaq temperaturunda kubik fəza qruplu simmetriyaya uyğun gəlir. Termofiziki tədqiqatlarda müəyyən olunmuşdur ki, TiNbCN örtüyünün termik keçidlər mürəkkəb mexanizimlə baş verir. DSC spectrinin kinetikasından təyin olunmuşdur ki, $T \leq 50$ °C sürətli parçalanma, $T \leq 270$ °C zəyif parçalanma və $T \leq 600$ °C sürətli parçalanma hissələrindən ibarətdir. Həmçinin DSC kinetikasından müəyyən edilmişdir ki, 565 °C temperaturda faza keçidi baş verir.

Açar sözlər: örtük materiallar, istilik axını funksiyası, kristal quruluş, faza analizi, DSC.